Chem Soc Rev

RSC Publishing

TUTORIAL REVIEW

Sonochemical synthesis of nanomaterials†

Hangxun Xu, Brad W. Zeiger and Kenneth S. Suslick*

Cite this: *Chem. Soc. Rev.*, 2013, **42**, 2555

Received 26th July 2012

DOI: 10.1039/c2cs35282f

www.rsc.org/csr

High intensity ultrasound can be used for the production of novel materials and provides an unusual route to known materials without bulk high temperatures, high pressures, or long reaction times. Several phenomena are responsible for sonochemistry and specifically the production or modification of nanomaterials during ultrasonic irradiation. The most notable effects are consequences of acoustic cavitation (the formation, growth, and implosive collapse of bubbles), and can be categorized as primary sonochemistry (gas-phase chemistry occurring inside collapsing bubbles), secondary sonochemistry (solution-phase chemistry occurring outside the bubbles), and physical modifications (caused by high-speed jets or shock waves derived from bubble collapse). This *tutorial review* provides examples of how the chemical and physical effects of high intensity ultrasound can be exploited for the preparation or modification of a wide range of nanostructured materials.

1. Introduction

High intensity ultrasound has found many important applications in organic synthesis, materials and organometallic chemistry, and industrial manufacturing processes.[1–9] Sonochemistry originates from the extreme transient conditions induced by ultrasound, which produces unique hot spots that can achieve temperatures above 5000 K, pressures exceeding 1000 atmospheres, and heating and cooling rates in excess of 10^{10} K s^{-1}.[4,10] These conditions are distinct from other conventional synthetic techniques such as photochemistry, wet chemistry, hydrothermal synthesis, or flame pyrolysis (Fig. 1).[2–4,11]

The speed of sound in a typical liquid is 1000 to 1500 m s^{-1}, and ultrasonic wavelengths will vary from roughly 10 cm down to 100 μm over a frequency range of 20 kHz to 15 MHz, much larger than the molecular size scale. The chemical and physical effects of ultrasound therefore arise *not* from a direct interaction between chemical species and sound waves, *but rather from the physical phenomenon of acoustic cavitation*: the formation, growth, and implosive collapse of bubbles.[11–13] When sound waves with sufficient amplitude propagate through a liquid, the liquid is

Department of Chemistry, University of Illinois at Urbana-Champaign, 600 South Mathews Ave., Urbana, Illinois 61801, USA. E-mail: ksuslick@illinois.edu; Fax: +1 217 333 2685; Tel: +1 217 333 2794

† Part of the chemistry of functional nanomaterials themed issue.

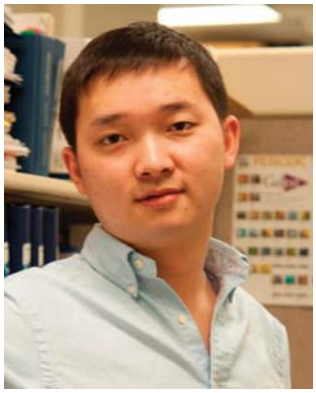

Hangxun Xu

Hangxun Xu was born in Zhejiang, China, in 1983. He obtained his BS degree in polymer chemistry from the University of Science and Technology of China (USTC) in 2006. He then came to the United States and received his PhD in chemistry (2011, under the supervision of Prof. Kenneth S. Suslick) at the University of Illinois at Urbana-Champaign and is now a postdoctoral research associate with Prof. John A. Rogers.

Brad W. Zeiger

Brad Zeiger received his BS in chemistry from Western Washington University in 2007, where he studied complexes of group VI metals with catecholate ligands. He is currently pursuing his PhD in inorganic chemistry at the University of Illinois at Urbana-Champaign. His research has focused on the physical and chemical effects of ultrasound, with specific interests including sonocrystallization, ultrasonic processing of molecular crystals, and time-resolved single-bubble sonoluminescence.

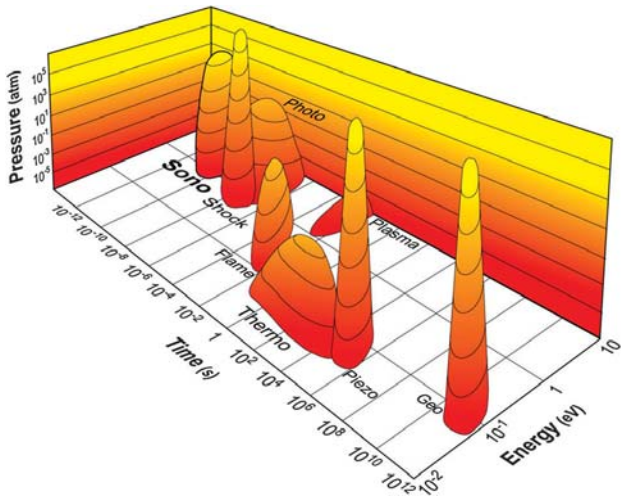

Fig. 1 Islands of chemistry as a function of time, pressure, and energy. Sonochemistry occupies a unique short-time, high-energy, and high-pressure space. Reprinted with permission from ref. 10. Copyright 2008 Annual Reviews.

under dynamic tensile stress and the density changes with alternating expansive and compressive waves. Bubbles will be generated from pre-existing impurities (*e.g.*, gas-filled crevices in dust motes) and oscillate with the applied sound field. As illustrated in Fig. 2, bubbles can grow through a slow pumping of gas from the bulk liquid into the oscillating bubble (rectified diffusion). Bubbles at a critical size (usually tens of micrometres) can couple strongly to the acoustic field and undergo a rapid inertial overgrowth during expansion, followed by a catastrophic collapse. The implosive collapse process is nearly adiabatic in its final stages and is responsible for the extreme conditions characteristic of sonochemistry.

The extreme, transient conditions produced during acoustic cavitation allow the formation of unique materials and also permit syntheses on the benchtop in a room-temperature liquid that would otherwise require high temperatures, high pressures, or long reaction times. When a liquid is irradiated by high

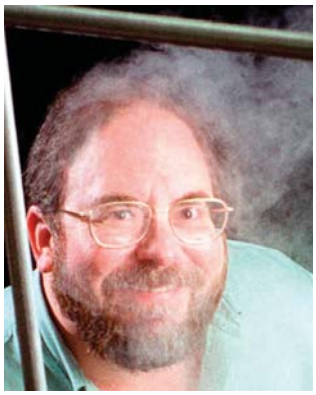

Kenneth S. Suslick

Ken Suslick is the Marvin T. Schmidt Professor of Chemistry at the University of Illinois at Urbana-Champaign. Professor Suslick received his BS from Caltech in 1974, PhD from Stanford in 1978. Suslick is the recipient of the Sir George Stokes Medal of the Royal Society of Chemistry, the ACS Nobel Laureate Signature Award for Graduate Education, the MRS Medal, the ACS Senior Cope Scholar Award, the Mentorship Award of the ASA, a Guggenheim Fellowship, and the Silver Medal of the Royal Society for Arts. He is a Fellow of the AAAS, ACS, MRS and ASA.

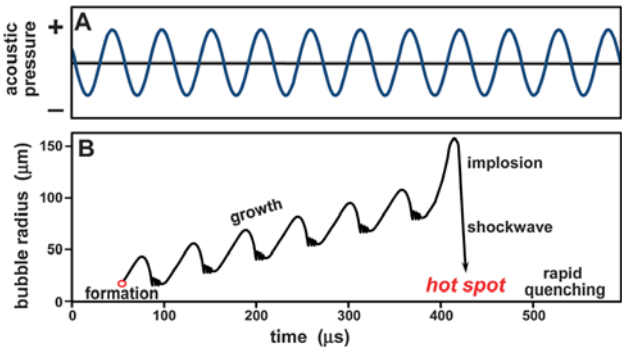

Fig. 2 Schematic illustration of the process of acoustic cavitation: the formation, growth and implosive collapse of bubbles in a liquid irradiated with high intensity ultrasound.

intensity ultrasound, high-energy chemical reactions occur. Sonochemistry can be employed in the synthesis of materials from volatile or nonvolatile precursors, but generally through different mechanisms (Fig. 3). In the former case, the volatile precursor (*e.g.*, a volatile organometallic compound) will produce free metal atoms generated by bond dissociation due to the high temperatures created during bubble collapse. These atoms can be injected into the liquid phase and nucleate to form nanoparticles or other nanostructured materials if appropriate templates or stabilizers are present in the solution. Nonvolatile precursors may still undergo sonochemical reactions, even outside of the collapsing bubbles by undergoing reactions with radicals or other high energy species produced from the sonolysis of vapour molecules inside the collapsing bubbles that then diffuse into the liquid phase to initiate a series of reactions (*e.g.*, reduction of metal cations).

The physical effects induced by high intensity ultrasound are also often accompanied by chemical consequences and find increasingly frequent use in materials synthesis. A trivial example is the simple heating of the bulk liquid: typical laboratory scale ultrasonic horns (Fig. 4) deliver roughly 10 to 100 watts of

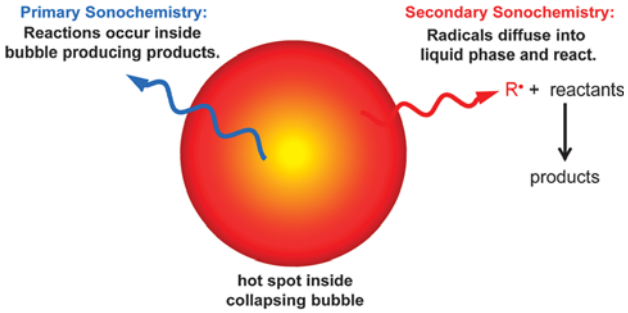

Fig. 3 Primary sonochemistry and secondary sonochemistry for preparation of nanomaterials. An example of primary sonochemistry is the generation of metal atoms from sonolysis of weak metal–carbon bonds from volatile organometallic compounds inside the collapsing bubble that then diffuse into the bulk liquid to form functional nanomaterials. Secondary sonochemical products may arise from chemically active species (*e.g.*, organic radicals from sonolysis of vapour) that are formed inside the bubble, but then diffuse into the liquid phase and subsequently react with solution precursors to form a variety of nanostructured materials.

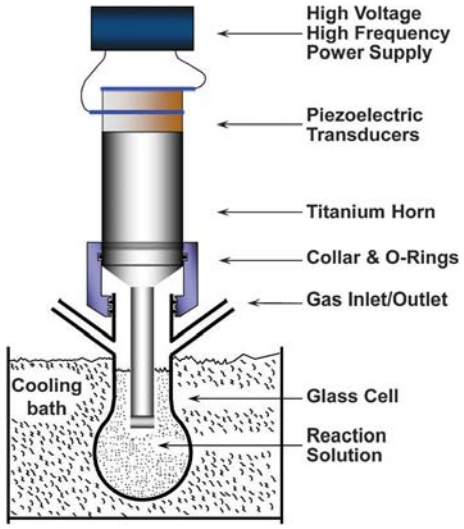

Fig. 4 A typical laboratory rig for sonochemical reactions uses a high intensity ultrasonic horn, typically around 20 kHz and 10 to 100 W acoustic power. Reprinted with permission from ref. 3. Copyright 2010 John Wiley & Sons.

acoustic energy into the liquid during sonication. This ultrasonic power output must be calibrated, most commonly by calorimetry, in order to accurately report experimental conditions, but unfortunately many researchers overlook this critical parameter. A common alternative to ultrasonic horns, ultrasonic cleaning baths, are common in research labs and are easily obtained. The actual ultrasonic power density of an ultrasonic cleaning bath is typically only a few percent of that generated by an ultrasonic horn. Cleaning baths are often marginal for many sonochemical reactions, but can be useful for the physical effects of ultrasound, *e.g.*, for activating highly reactive metals (*e.g.*, Li or Mg), generating emulsions, accelerating dissolutions of solids, facilitating crystallizations, and exfoliating layered materials.

The most important physical phenomena for the preparation or modification of nanomaterials are microjets and shock waves. Microjets occur when bubbles collapse near an extended surface (*i.e.*, surfaces several times larger than the bubble radius).[14] The inhomogeneity of the bubble's surroundings induces an asphericity into the bubble, which self-reinforces during collapse; this is similar to a shaped-charge explosive. These high speed microjets impact on the surface and can cause pitting and erosion of surfaces leading to modification of surfaces and generation of surface nanostructures.

If the bubble is unperturbed by a surface, then the rapid rebound from its minimum radius is spherical. The compression of the surrounding liquid propagates outward as a shock wave from the rebounding bubble. A shock wave generated from a laser-induced collapsing bubble is shown in Fig. 5.[15] Such shocks can reach pressures of 60 kbar and velocities of 4 km s^{-1} in water. These shock waves can induce several different physical effects with chemical consequences, including enhanced mass transport due to strong turbulent mixing and acoustic streaming. In addition, shock waves can accelerate solid particles suspended in the liquid. Interparticle collisions can reach velocities of hundreds of metres per second, causing changes in particle size

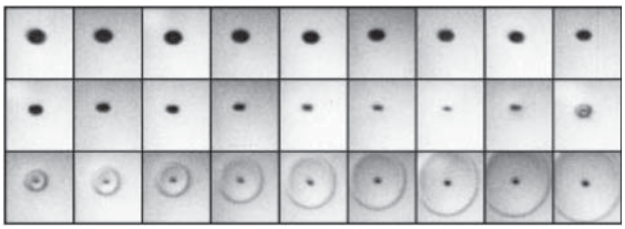

Fig. 5 A spherical shock wave launched from a laser-induced collapsing bubble. The shock wave can reach 60 kbar with velocities of 4 km s^{-1}. Images were acquired at a shutter speed of 20.8 million frames per second, frame size was 1.5 × 1.8 mm^2, and the exposure time was 5 ns. Reprinted with permission from ref. 15. Copyright 1999 The Royal Society.

distributions, particle morphologies, and surface compositions.[16,17] Particle agglomeration (for malleable materials), particle fragmentation (for brittle materials) and exfoliation of layered materials into 2D layers have all been observed.[2,3,9]

The applications of high intensity ultrasound to materials chemistry are diverse and rapidly increasing. Fig. 6 gives a broad organizational schema for sonomaterials research to date. In this *tutorial review*, we provide a sampling of the most important and most recent results of sonochemical applications to nanomaterials synthesis and preparation. We have organized the review based on the chemical or physical effect of ultrasound exploited for the formation of nanomaterials: (1) primary sonochemistry employing volatile precursors, (2) secondary sonochemistry using non-volatile precursors, (3) materials created or modified through the physical effects of ultrasound (*i.e.*, shock waves), and (4) materials in which both chemical and physical effects of ultrasound have a synergistic impact.

2. Chemical effects of ultrasound for nanomaterials preparation

A. Nanomaterials prepared from volatile precursors

Ultrasonic irradiation of volatile organometallic compounds such as $Fe(CO)_5$ or $Cr(CO)_6$ in a nonvolatile solvent (*e.g.*, silicone oil or long-chain hydrocarbons) results in dissociation of the metal-carbonyl bonds and release of individual elemental metal atoms.[18] These atoms will be thermally excited to the point that they emit visible light analogous to emission from flame excitation and their atomic emission lines have been used to characterize the bubble conditions.[19] Nonvolatile solvents are necessary because additional vapour, especially of polyatomics, absorbs the available energy in the collapsing bubble (*via* rotational and vibrational molecular modes, ionization, and competing bond dissociation) and the conditions achieved are much less extreme. Control of surfactants, supports, or other reactants provides a facile route to a variety of metallic nanomaterials (Fig. 7).[2]

Nanostructured metal particles were the first demonstration of the application of chemical effects of high intensity ultrasound for the preparation of nanomaterials.[20] Ultrasonic irradiation of solutions containing volatile organometallic compounds such as $Fe(CO)_5$, $Ni(CO)_4$, and $Co(CO)_3NO$ produced porous, coral-like

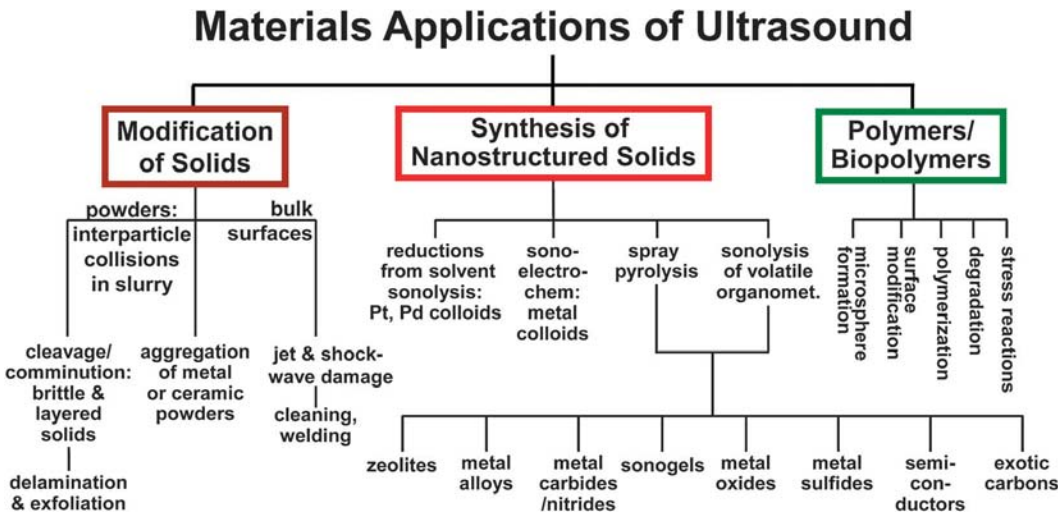

Fig. 6 The applications of sonochemistry to materials are diverse and rapidly expanding.

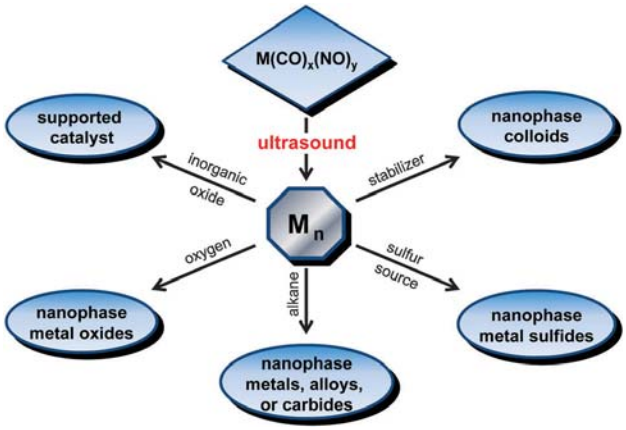

Fig. 7 The sonochemistry of volatile organometallics provides a versatile route to a variety of nanostructured materials. Reprinted with permission from ref. 3. Copyright 2010 John Wiley & Sons.

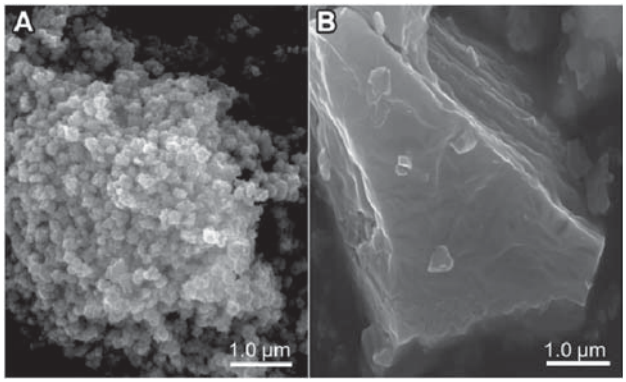

Fig. 8 SEM images of (A) sonochemically synthesized MoS_2 and (B) conventional MoS_2. Reprinted with permission from ref. 25. Copyright 1998 American Chemical Society.

aggregates of amorphous metal nanoparticles.[20,21] A classic example of this is the sonication of $Fe(CO)_5$ in decane at 0 °C under Ar, which yielded a black powder. The material was >96% iron, with a small amount of residual carbon and oxygen present from the solvent and CO ligands. SEM images revealed that the powder was an agglomerate of 20 nm iron particles. If surfactants such as oleic acid or polyvinylpyrrolidone were present in the solvent to stabilize the particles then individual iron nanoparticles were produced.[22] These iron nanoparticles had a diameter of ~8 nm and were amorphous (measured by electron diffraction).[22] Magnetic studies indicated that these iron nanoparticles were superparamagnetic. Bimetallic alloy particles have also been prepared in this way. For example, sonication of $Fe(CO)_5$ and $Co(CO)_3NO$ led to the formation of Fe–Co alloy particles.[23,24] The composition was controllable by varying the ratio of the precursors in the solution. Alloy nanoparticles typically exhibit superior catalytic properties compared to monometallic nanoparticles.

The metal atoms decomposed from organometallic compounds during sonication are highly reactive and can react with other chemical substances in the solvent to form new materials. Nanostructured MoS_2, for example, was synthesized by the sonication of $Mo(CO)_6$ with elemental sulphur in 1,2,3,5-tetramethylbenzene under Ar.[25] MoS_2 prepared sonochemically differs dramatically in morphology from conventional MoS_2: conventional MoS_2 is a layered, plate-like material, while sonochemically synthesized MoS_2 exhibited a spherical morphology with an average diameter of 15 nm (Fig. 8). TEM examination revealed that sonochemically prepared MoS_2 contained more defects and showed many more edges, although both MoS_2 materials had the same interlayer distance of 0.62 ± 0.01 nm. MoS_2 has been frequently used as a hydrodesulfurisation catalyst in the petroleum industry to remove sulphur from crude oil before combustion. Sonochemically prepared MoS_2 exhibited substantially higher catalytic activity than conventional MoS_2 for the hydrodesulfurisation of thiophene. The increase in catalytic activity was attributed to the higher surface area and more edges and defects found in the sonochemically prepared MoS_2.

The preparation of refractory nanomaterials remains problematic because most high temperature routes lead to agglomeration of

precursors or intermediate states during the synthesis. Sonochemical routes, however, produce the needed high temperatures on the nanoscale in the localized hot spots of the collapsing bubble. As a specific example, sonochemistry provides a convenient approach to prepare nanostructured metal carbides that exhibit excellent catalytic activity.[26,27] Mo_2C and W_2C are particularly interesting catalysts because they show catalytic activity similar to platinum group metals, but their syntheses are challenging because of the refractory nature of metal carbides. The sonication of $Mo(CO)_6$ or $W(CO)_6$ in hexadecane leads to the formation of amorphous metal oxycarbides. Removing oxygen by heating under 1 : 1 CH_4/H_2 leads to the formation of nanostructured Mo_2C or W_2C as porous aggregates of small nanoparticles with surface areas of 130 $m^2\ g^{-1}$ and 60 $m^2\ g^{-1}$ for Mo_2C and W_2C, respectively. They exhibit activities and selectivities similar to platinum for dehydrogenation reactions.[26] In addition, these nanostructured metal carbides show superior activity, selectivity, and stability for the hydrodehalogenation of organic pollutants.[27] Metal nitrides can also be prepared by the sonication of metal carbonyl compounds under a reductive gas mixture of NH_3 and H_2 at 0 °C.[28]

When a sacrificial template (*e.g.*, microspheres of silica or carbon) is present in the sonicated solution, the free metal atoms produced by ultrasonic irradiation of volatile organometallic compounds can deposit onto the template to form different structured materials. For example, ultrasonic irradiation of $Mo(CO)_6$, sulphur, and silica nanoparticles in isodurene under Ar forms MoS_2-coated silica nanoparticles.[29] Replacing Ar with air and removing sulphur from the system yields MoO_3-coated silica nanoparticles. Etching of the silica component by HF leaves hollow MoS_2 or MoO_3. These hollow MoS_2 nanoparticles had better catalytic activity toward the hydrodesulfurization of thiophene than even sonochemically prepared MoS_2 nanoparticles due to the significantly increased number of edge defects and improved accessibility to both inner and outer surfaces of the hollow structures. Amusingly, the hollow MoO_3 spheres, which are initially amorphous, upon heating crystallize into *hollow single crystals*.[29]

Ultrasonic irradiation of $Fe(CO)_5$ in the presence of carbon nanoparticles provided a facile method for the preparation of hollow hematite.[30] Carbon nanoparticles were used as a template that spontaneously removes itself through combustion induced by the rapid oxidation of the outer Fe shell upon exposure to air. Porous Co_3O_4 was produced in a similar fashion when carbon nanotubes were used as the template and $Co_4(CO)_{12}$ as the precursor.[31] Co_3O_4 prepared in this way was found to be an excellent electrode material for lithium-ion batteries.

A sonochemical method has also been used to synthesize single-walled carbon nanotubes *via* ultrasonic irradiation of a solution containing silica powder, ferrocene, and *p*-xylene (Fig. 9).[32] In this synthesis, ferrocene was used as the precursor for the Fe catalyst, *p*-xylene was used as a carbon precursor, and silica powder provided nucleation sites for the growth of carbon nanotubes. Ferrocene was sonochemically decomposed to form small Fe clusters and *p*-xylene was pyrolyzed to carbon atoms and carbon moieties. This approach provides a convenient synthetic route for the preparation of carbon nanotubes under ambient conditions. In addition, no extra purification steps were needed in this process, which opens up the possibility for large-scale ultrasonic synthesis of high-purity, single-walled carbon nanotubes.

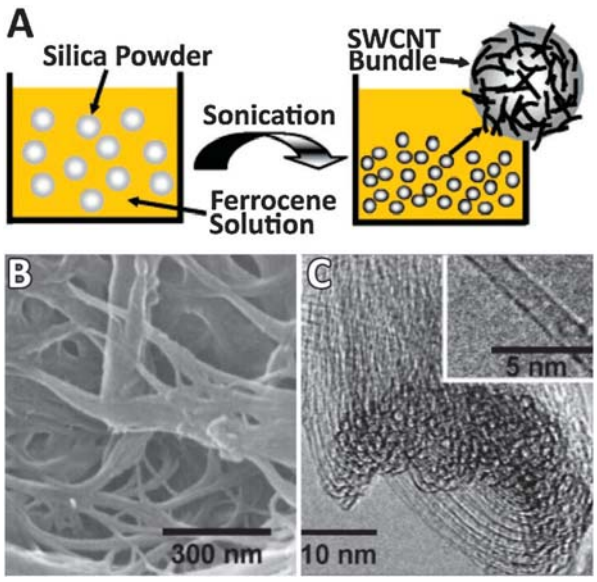

Fig. 9 (A) Schematic illustration of the sonochemical preparation of single-walled carbon nanotubes on silica powders. (B) SEM image of carbon nanotube bundles on polycarbonate filter membrane. (C) HRTEM images of single-walled carbon nanotubes within the bundles. Reprinted with permission from ref. 32. Copyright 2004 American Chemical Society.

Ultrasonic irradiation of common organic solvents such as $CHCl_3$, CH_2Cl_2, and CH_3I with HF-etched Si nanowires yielded hydrocarbon materials with diverse structures (*e.g.*, nanotubes and nano-onions).[33] The nanostructured SiH_x on the Si nanowires served as a template for the nucleation of carbon species formed from the pyrolysis of volatile organics inside the collapsing bubbles.

B. Nanomaterials prepared from nonvolatile precursors

Sonochemistry is also commonly used to prepare nanostructured noble metals when nonvolatile precursors are dissolved in a volatile solvent (usually water or alcohols). In these cases, sonolysis of the solvent vapour produces strong reductants that have a number of advantages over traditional reduction techniques: no additional reducing agents are required, the reduction rate is generally very fast, and very small nanoclusters can be made in this way when suitable stabilizers are present.

Ultrasonic irradiation of water generates highly reactive $H^\bullet$ and $OH^\bullet$ radicals which are responsible for redox chemistry. These reactive radicals can further react with organic additives (*e.g.*, 2-propanol or ethanol) in the solution to generate secondary radicals ($R^\bullet$) which can dramatically promote the reduction rate. Overall, the process (including competing reactions) can be summarized as follows:

$$H_2O \rightarrow H^\bullet + OH^\bullet \quad (1)$$

$$H^\bullet + H^\bullet \rightarrow H_2 \quad (2)$$

$$H^\bullet + OH^\bullet \rightarrow H_2O \quad (3)$$

$$OH^{\bullet} + OH^{\bullet} \rightarrow H_2O_2 \quad (4)$$

$$RH\ (\text{volatile vapour}) \rightarrow R^{\bullet} + H^{\bullet} \quad (5)$$

$$RH + OH^{\bullet}\ (\text{or } H^{\bullet}) \rightarrow R^{\bullet} + H_2O\ (\text{or } H_2) \quad (6)$$

$$M^{n+} + nR^{\bullet}\ (\text{or } H^{\bullet}) \rightarrow M^0 \quad (7)$$

$$mM^0 \rightarrow M_m\ (M = \text{noble metal}) \quad (8)$$

Unlike metallic particles prepared from the sonication of volatile organometallic compounds, which are typically amorphous, materials produced from nonvolatile compounds are usually well crystallized.

Nanostructured noble metals (*e.g.*, Au, Ag, Pt, and Pd) can be prepared by a large number of synthetic routes, including controlled chemical reduction, solvothermal synthesis, photochemical reduction, and radiolytic reduction. Sonochemical preparation also provides a facile approach for the production of spherical metal nanoparticles.[34–40] A systematic study carried out by Grieser *et al.* on the effect of ultrasound on the synthesis of noble metal nanoparticles has shown that the particle size is largely determined by solvent/surfactant properties: particle size is inversely related to alcohol concentration and alkyl chain length.[34] This observation led to the conclusion that alcohol molecules adsorbed to the surface of nuclei can limit the growth of small nanoparticles. The other possible explanation for this result is that more secondary radicals can form at higher alcohol concentrations which leads to faster reduction rates which in turn results in smaller and possibly more uniform particles.

Sequential sonochemical reduction of two different metallic ions will result in bimetallic core–shell nanoparticles. For example, the sonochemical reduction of a solution containing both Au(III) and Pd(II) ions led to the formation of nanoparticles with a Pd shell over an Au core.[35] The core–shell structure is a result of the difference in reduction potential between Pd(II) and Au(III) ions. When Au and Pd nanoparticles are formed simultaneously, excess Au(III) ions will oxidize Pd nanoparticles to form Au and Pd(II) ions. The Pd shell can only form once the gold ions have all been reduced into nanoparticles. A similar approach can be used to sonochemically prepare Au/Ag and Pt/Ru core–shell particles.[36,37]

Sonochemical methods have also been developed to prepare nonspherical nanoparticles. For example, gold nanorods have been synthesized by the sonochemical reduction of $HAuCl_4$ in the presence of $AgNO_3$, CTAB, and ascorbic acid.[38] The solution pH influences the aspect ratio of the gold nanorods: as the pH of the solution increases, the average aspect ratio of the gold nanorods decreases. Ultrasound-induced reduction of $HAuCl_4$ onto pre-synthesized gold seeds using polyvinylpyrrolidone (PVP) as a stabilizing polymer leads to the formation of monodispersed gold nanodecahedra.[39] This sonochemical method can significantly increase the yield and reproducibility. Ag nanoplates have also been synthesized by a similar ultrasound-assisted Ostwald ripening process using Ag nanoparticles as seeds.[40] These platelike nanostructures served as templates to fabricate ringlike metal structures *via* a simple displacement reaction under ultrasonic irradiation. Ag nanowires and nanorods have also been prepared by sonicating suitable Ag precursors.

Polymers or small molecules can act as structure directing agents as well as stabilizers. Ultrasonic irradiation of $HAuCl_4$ solution containing α-D-glucose produced gold nanobelts with a width of 30–50 nm and a length of several micrometres.[41] These gold nanobelts are formed through 3 steps: (1) formation of gold nanoparticles *via* sonochemical reduction, (2) aggregation and room-temperature temperature sintering of gold nanoparticles directed by α-D-glucose, and (3) further growth along the Au[111] direction with recrystallization finally yielding the isolated single-crystalline gold nanobelts.

Highly fluorescent, stable, and water-soluble Ag nanoclusters (diameter less than 2 nm) have been successfully prepared by sonication of aqueous $AgNO_3$ solutions with dissolved polymethylacrylic acid (PMAA) (Fig. 10).[42] The charged carboxylate groups of PMAA can stabilize clusters of Ag atoms in solution and prevent further growth of nanoclusters to form large nanoparticles. The optical and fluorescence properties of these Ag nanoclusters can be controlled by varying synthetic conditions, *e.g.*, sonication time, stoichiometry of the carboxylate groups relative to Ag^+, and the polymer molecular weight. Ag nanoclusters, as a new kind of nanoparticle fluorophore, are likely to find widespread applications in bioimaging, chemical and biosensing and single-molecule studies.

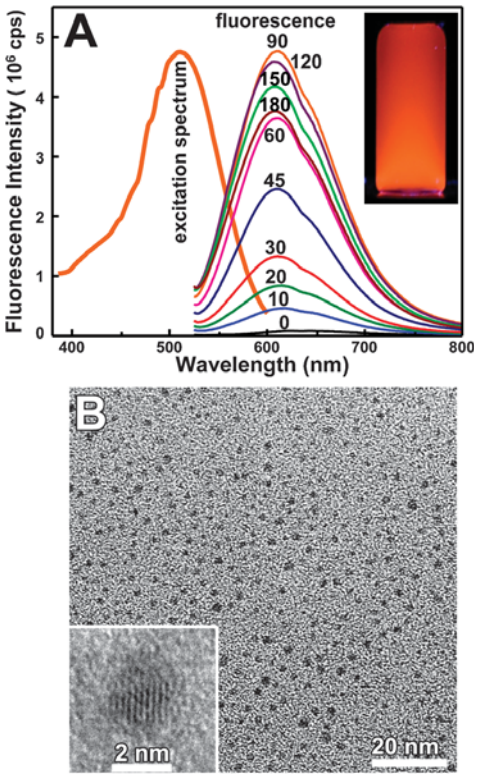

Fig. 10 (A) Fluorescence emission spectra of Ag nanoclusters prepared by the sonochemical method with different durations of sonication time, indicated in minutes (inset: vial containing a solution of the Ag nanoclusters illuminated by a 365 nm UV lamp). (B) TEM images of as-prepared Ag nanoclusters after 90 min sonication (inset shows a single magnified Ag nanocluster). Reprinted with permission from ref. 42. Copyright 2010 American Chemical Society.

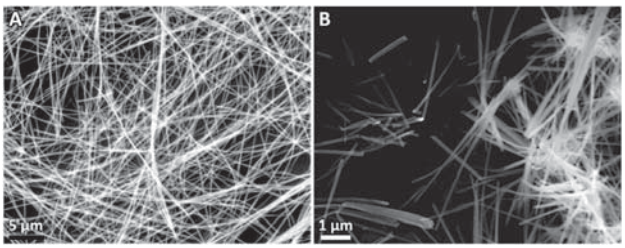

Fig. 11 SEM images of (A) typical trigonal Se nanowires synthesized by sonication of amorphous selenium grown in ethanol at room temperature and (B) grown from amorphous Se colloids in ethanol without sonication. Reprinted with permission from ref. 43. Copyright 2003 American Chemical Society.

The sonochemical reduction of nonvolatile precursors in solution is not limited to noble metals. For example, trigonal Se nanowires were prepared by the sonication of amorphous Se colloids in alcohol solvents without templates or surfactants (Fig. 11).[43] Nanocrystals of trigonal Se were nucleated sonochemically and acted as seeds for the growth of Se nanowires through a solid-solution-solid transformation mechanism driven thermodynamically: amorphous Se has a higher free energy than trigonal Se.

Various metal oxides and metal chalcogenides have also been prepared by sonochemical methods with nonvolatiles.[44–46] A typical synthesis of these types of materials involves the sonication of a solution containing a metal salt and an oxygen or chalcogen source (*e.g.*, air for oxygen, thiourea for sulphur, selenourea for selenium, or sometimes, a sulphate or selenate). Reactive species such as reactive radicals or atoms ($O^{\bullet}$ or $S^{\bullet}$) can react with metal ions in the solution to form metal oxides or metal chalcogenides. If proper structure directing agents are used, different nanostructured materials (*e.g.*, hollow spheres, nanorods, nanowires, or nanocubes) can be obtained. For example, ultrasonic irradiation of $CdCl_2$, $NaSeSO_3$, and ammonia leads to the formation of hollow CdSe spheres.[44] $CdCl_2$ was hydrolysed under the basic conditions to form $Cd(OH)_2$ which acted as an *in situ* template for the sonochemical formation of hollow structures. This process can be written as follows:

$$H_2O \rightarrow H^{\bullet} + OH^{\bullet} \quad (9)$$

$$2H^{\bullet} + SeSO_3^{2-} \rightarrow Se^{2-} + 2H^{+} + SO_3^{2-} \quad (10)$$

$$Cd(OH)_2 + Se^{2-} \rightarrow CdSe + 2OH^{-} \quad (11)$$

$$n\mathrm{CdSe} \rightarrow (\mathrm{CdSe})_n \quad (12)$$

Hetero-structured materials such as core–shell SnO_2/CdS and ZnO/CdS have also been prepared *via* sonochemical deposition of metal sulphide onto metal oxides.[45] In a similar fashion, by exploiting the hydrogen radicals formed from sonolysis of water vapor inside the collapsing bubbles, copper hydride (CuH) can be produced *via* ultrasonic irradiation of a copper(II) aqueous solution.[46]

As a synthetic tool, sonochemistry can deposit nanoparticles formed *in situ* onto pre-existing substrates (*e.g.*, polystyrene spheres, silica particles, carbon nanotubes, or a polymer matrix).[47–49] Graphene has emerged as a new 2D material with unique electrical, thermal, and mechanical properties. Catalyst assemblies of nanostructured materials with exfoliated, single-layer graphene (often prepared sonochemically, as discussed later) have shown great promise for a wide range of applications including sensors, fuel cells, lithium-ion batteries, photocatalysts, and fuel cells. Ultrasonic irradiation of graphene oxide with $HAuCl_4$ in water produced well-dispersed reduced graphene oxide/Au composites by simultaneous or sequential reduction procedures.[50] The formation of reactive $OH^{\bullet}$ and $H^{\bullet}$ radicals *via* sonolysis of water vapour inside collapsing bubbles is responsible for the formation of reduced graphene oxides and the reduction of Au(III) to Au nanoparticles (eqn (1)–(7)).

Aligned nanostructures can be achieved with the help of ultrasound. For example, vertically aligned ZnO nanorods were prepared on substrates such as Zn sheets, Si wafers, glass, and polycarbonate membranes by sonicating a precursor solution containing Zn^{2+}.[51] Ultrasonic irradiation rapidly induces the anisotropic growth of ZnO along the (0001) direction on the substrate. The alignment is presumed to be due in part to the relative depletion of Zn^{2+} concentration at the base of the growing rods relative the tops of the rods. Oxygen atoms, hydroxyl radicals or hydroperoxyl (HO_2) radicals formed by the sonication of water in air are thought to be responsible for the formation of these ZnO rods. Compared to a conventional hydrothermal process, the growth rate of ZnO is increased by 10 fold, with an average growth rate of $\sim$500 nm h^{-1}.

3. Physical effects of ultrasound for nanomaterials synthesis

The most important physical effects of high intensity ultrasound arise from the high-speed jets and intense shock waves induced by cavitation. They have been frequently used to prepare emulsions, agglomerate malleable materials, break down friable materials, modify solid surfaces, and exfoliate layered materials. Enhanced mass transfer as a consequence of acoustic streaming and bulk thermal heating are other physical effects of high intensity ultrasound.

A good example of exploiting the physical effects of ultrasound is the enhancement of intercalation of guest substances into layered materials first developed by Green, Suslick and co-workers.[52] In more recent work, graphite, with its layered planar structure, can accommodate in between each graphene layer guest molecules or atoms to form graphite intercalation compounds, but the formation of intercalation compounds is usually a very slow process. Ultrasonic irradiation, however, can dramatically increase the reaction rate.[53] For example, potassium intercalated compounds (KC_8) can be prepared by the sonication of graphite with potassium under an Ar atmosphere in 3 minutes while normal preparation methods require 1–8 hours *via* a solid state reaction at high temperature under an inert atmosphere. H_2PtCl_6 can also be intercalated into graphite layers to prepare Pt nanoparticles intercalated in graphite after exposure to an H_2 gas stream.[54] The sonication of potassium intercalated graphite in ethanol can generate carbon nanoscrolls (Fig. 12).[55]

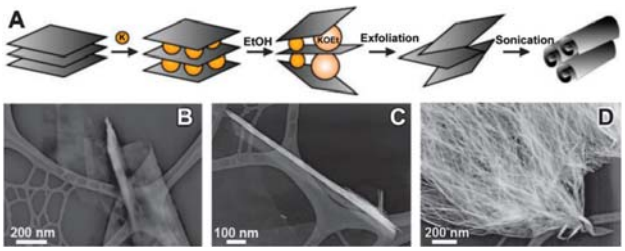

Fig. 12 (A) Schematic illustration of the intercalation and exfoliation process to prepare carbon scrolls. TEM images of (B) a thin layer of graphite sheets in the process of scrolling, (C) an isolated carbon nanoscrolls with open ends, and (D) a bundle of scrolled carbon nanosheets. Reprinted with permission from ref. 55. Copyright 2003 AAAS.

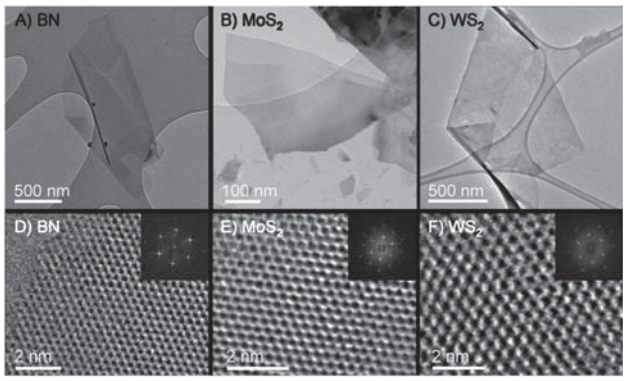

Fig. 13 TEM images of individual nanosheets. (A to C) Low-resolution TEM images of flakes of BN, MoS_2, and WS_2, respectively. (D to F) High-resolution TEM images of BN, MoS_2, and WS_2 monolayer (Insets) Fast Fourier transforms of the images. Reprinted with permission from ref. 57. Copyright 2011 AAAS.

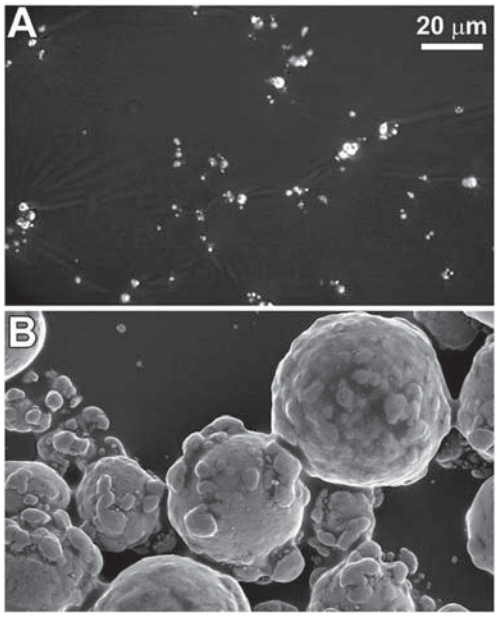

Fig. 14 Effects of ultrasonic irradiation on slurries of fine Zn powder (5 μm diameter, roughly spherical). (A) SEM before ultrasonic irradiation. (B) Dense agglomeration after 90 min sonication of 2% w/w decane slurry at 20 kHz, 50 W cm^{-2}, 283 K, where agglomerates are made from ~1000 of the initial particles and loadings up to 50% w/w show similar results. The same magnification is used in both images. Reprinted with permission from ref. 17. Copyright 2004 American Chemical Society.

The conversion efficiency is very high, up to ~80%, compared to a reaction in the absence of ultrasound, which results in very few nanoscrolls. The reason for the formation of carbon nanoscrolls is not fully understood, but ultrasound provides the necessary mechanical energy to overcome the van der Waals force between each graphene layer. The individual exfoliated graphene layers can then fold *via* intralayer interactions to reach a stable structure in the solvent.

Ultrasound has become a formidable tool for the chemical preparation of single and few layer graphene. In a typical synthesis of graphene oxide, pristine graphite is oxidized by Hammer's method to form graphite oxide, which has an increased interlayer distance relative to graphite and the van der Waals force is consequently weaker. After mild sonication (*e.g.*, bath sonication is sufficient), single-layered graphene oxides can be produced which can then be chemically reduced to graphene. A more straightforward method for the preparation of graphene is the direct liquid-phase exfoliation of graphite by sonication. To obtain high yields of exfoliated graphenes from graphite, the surface energy of the solvent must match the surface energy of graphite, 40–50 mJ m^{-2}. Sonication of graphite in suitable solvents (*e.g. N*-methyl-pyrrolidone (NMP)) can lead to the formation of single layer and few-layer graphenes.[56] Ultrasound is also frequently used to disentangle single-walled carbon nanotubes, which usually form bundles due to the van der Waals force.

This approach can be generalized to other layered materials such as $MoSe_2$, $MoTe_2$, MoS_2, WS_2, $TaSe_2$, $NbSe_2$, $NiTe_2$, BN, and Bi_2Te_3, all of which can be exfoliated in the liquid phase to prepare single-layered nanosheets (Fig. 13).[57] Ultrasound is a broadly useful tool for overcoming the attractive forces between individual layers to break 3D layer-structured materials down to 2D planar structures.

The impact of ultrasonic shock waves on pre-existing particles in a liquid is also an interesting use of the physical effects of ultrasound. For instance, high intensity ultrasound can drive metal microparticles suspended in liquid slurries into one another at high speeds (hundreds of metres per second) to induce local melting at the point of collision and consequent agglomeration (Fig. 14).[16,17] This can only happen with metals with relatively low melting point (*e.g.*, Sn, Zn, Cr, and barely Mo). If the melting points of the metal is higher than ~3000 K, no melting at the point of impact occurs. Furthermore, agglomeration of metal particles occurs only over a fairly narrow range of radius in the regime of a few microns. Neither particles too large nor too small will be accelerated to a sufficient velocity to induce local melting and consequent agglomeration (Fig. 15).

Such interparticle collisions during ultrasonic irradiation of slurries of high temperature superconductors can significantly improve their properties.[58,59] For example, the superconducting properties of $Bi_2Sr_2CaCu_2O_{8+x}$ are significantly improved after sonication as a slurry in decane due to the enhancement of intergrain coupling resulting from interparticle collisions.[58] Intergrain coupling controls the critical magnetic field (J_c) that limits the fields that can be formed with $Bi_2Sr_2CaCu_2O_{8+x}$ superconductors.

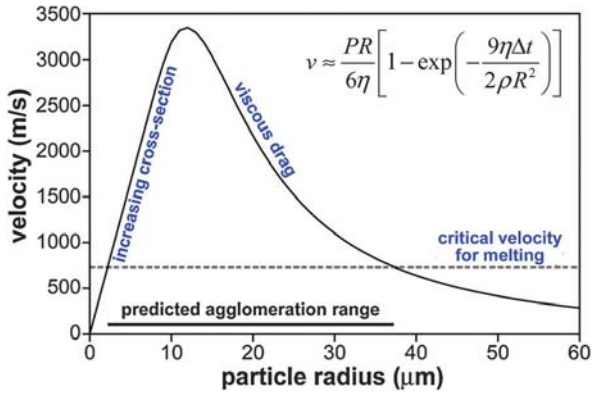

Fig. 15 Calculated velocities of interparticle collisions of Zn powder during ultrasonic shock waves as a function of particle radius. The critical velocity necessary for collisional agglomeration determines the particle size range over which agglomeration will occur. Reprinted with permission from ref. 17. Copyright 2004 American Chemical Society.

Ultrasound can also be used to promote the diffusion of dopant ions into spherical nanoparticles. For example, high intensity ultrasound is used to prepare Mg^{2+} doped ZnO nanoparticles with tuneable photoluminescence (from yellow to blue, Fig. 16).[60] The quantum yield of these Mg^{2+} doped ZnO nanoparticles is very high, >60% under optimal conditions. XRD and HRTEM results indicate that no MgO phase exists in the ZnO nanoparticles. Ultrasonic irradiation of a slurry containing Au colloids and TiO_2 particles can lead to the formation of Au nanoparticles intercalated into a mesoporous TiO_2 structure which shows enhanced photocatalytic properties.[61]

The microjets and shock waves produced by high intensity ultrasound near solid surfaces can also cause physical changes on the surfaces of particles and substrates. For instance, high intensity ultrasound has been applied to improve anticorrosion surface coatings. Generally, even pure aluminium metal is coated by a few nm thick oxide layer. This layer is not able to protect fully against corrosion agents and is often not strongly adhered to the underlying metal. The corrosion protection and adhesion properties, however, can be improved *via* ultrasonic treatment.[62] After ultrasonic irradiation, the existing oxide layer is removed and a newly active oxide layer forms that has been shown to exhibit superior resistance to corrosion.

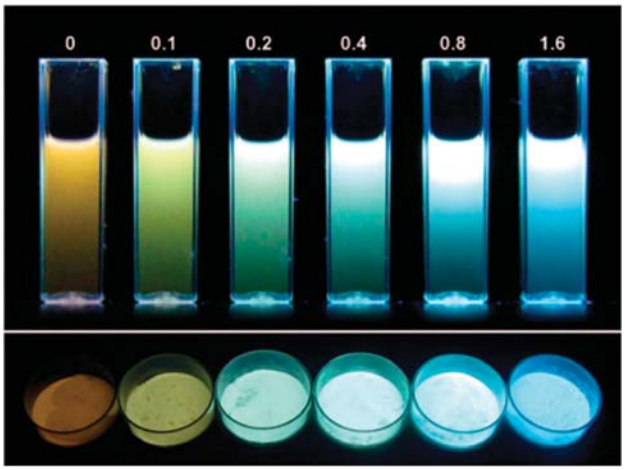

Fig. 16 Photographs (under UV light) of ethanol solutions (upper) and dry powders (lower) of Mg/ZnO nanoparticles prepared by ultrasonic irradiation of ZnO with Mg^{2+} with different Mg/Zn ratios. Reprinted with permission from ref. 60. Copyright 2009 John Wiley & Sons.

Ultrasonic irradiation can also improve sol–gel syntheses, a versatile technique for the preparation of nanostructured metal oxides. Application of ultrasound during a sol–gel process can accelerate the hydrolysis process and create metal oxides with narrower size distributions, higher surface area, and improved phase purity. For example, TiO_2, ZnO, CeO_2, MoO_3, V_2O_5, and In_2O_3 have all been prepared by the ultrasonic irradiation of their respective precursor solutions.[63,64] TiO_2 nanoparticles prepared by ultrasonic irradiation of the precursor solution are more photocatalytically active than commercial TiO_2 nanoparticles.[63] The increase in photocatalytic activity is attributed to the improved crystallinity of TiO_2 which is achieved due to accelerated hydrolysis under sonication.[63] Ultrasound can also induce the formation of unique morphologies during the synthesis of nanostructured metal oxides in the presence of soft templates. For example, hollow $PbWO_4$ spindles were prepared from the sonication of a solution of $Pb(CH_3COO)_2$, $NaWO_4$, and P123 (a Pluronic block copolymer, $EO_{20}PO_{70}EO_{20}$, M_{avg} = 5800).[65] In the absence of ultrasound, however, only solid particles were obtained. It was argued that ultrasound played an important role in the transformation of P123 micelles into hollow micelle aggregates which led to the formation of the hollow spindle structure.

The power of the physical effects of high intensity ultrasound is further illustrated by mechanochemical reactions of polymers, which include force-induced scission of covalent bonds. It has been well known since the 1950s that ultrasonic irradiation of solutions of high molecular weight polymers (both biomolecular and synthetic) results in chain scission and macroradical production.[66] More recently, the incorporation of mechanically sensitive chemical groups ("mechanophores") into a polymer chain has made it possible to illustrate the mechanical forces present during exposure to ultrasound.[67] Sonication accelerates rearrangement reactions with a bias towards reaction pathways that yield molecules not necessarily obtained from purely thermal or light-induced reactions.[67] For example, when 1,2-disubstituted benzocyclobutene is incorporated into a polymer chain and undergoes an ultrasonically-triggered electrocyclic ring opening process the same products are formed regardless of whether the original molecule was *cis* or *trans* (Fig. 17). If the reactions were initiated by light or heat alone, different products would form depending on the initial isomer. Thus, the mechanical force induced by ultrasound can alter the shape of the potential energy surfaces so that otherwise disfavored reactions can proceed under mild conditions. Ultrasound offers a way to access reaction pathways that may differ dramatically from those achieved by simply changing chemical or physical parameters. If stress-sensitive and cleavable groups are integrated in the polymer chain, sonication can result in the *precise* scission of the polymer chains. Some weak covalent

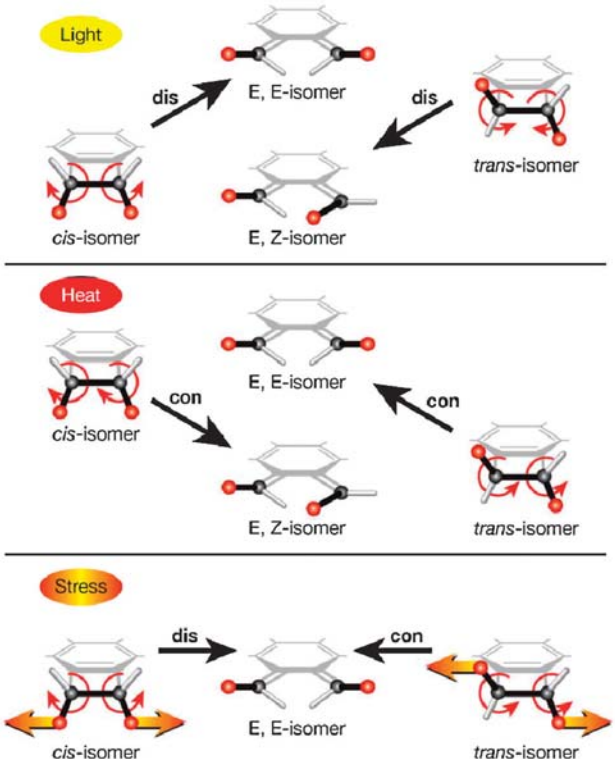

Fig. 17 Predicted intermediates of benzocyclobutene based on different activation mechanisms. Top: light activation induces only disrotary (dis) ring opening. Middle: heat activation induces only contrarotary (con) ring opening. Bottom: stress (ultrasound) causes dis or con ring opening depending on initial isomer. Reprinted with permission from ref. 67. Copyright 2007 Nature Publishing Group.

bonds such as peroxide and azo bonds, strained rings, and weak coordinative bonds (*e.g.*, palladium–phosphorus bonds) can be cleaved by ultrasound,[68–71] and even the click reaction can be unclicked within a polymer chain.[72]

Ultrasound also has effects on the process of crystallization (through increased nucleation, enhanced mass transport to the crystal surface, and sonofragmentation of larger crystals).[73] Sonication has been used to prepare nanostructured organic crystals, although reports of the formation of nanosized crystals in this area are uncommon; typical crystals produced in this way are of micron scale.[73] One example of the application of ultrasound to the preparation of nanocrystals is the preparation of cocrystals of 2(resorcinol)•2(4,4′-bpe), which can produce nanocrystalline cocrystals that exhibit single-crystal-to-single-crystal reactivity.[74] Compared with conventional reprecipitation methods, crystals obtained *via* sonochemistry were smaller and more uniform in size. Nanosized organic crystals of a self-assembled hexamer have also been prepared *via* an ultrasound-induced crystallization process. Nanosized hollow rhombic-dodecahedral crystals of the C-methylcalix[4]resorcinarene hexamer were achieved with rapid nucleation of a crystalline phase.[75] The mechanism for the formation of the hollow organic crystals is attributed to a reversed crystal growth mechanism heretofore described only in the synthesis of inorganic-based materials.

Broadly speaking, ultrasonic spray pyrolysis (USP) might also be regarded as an example of using physical effects of ultrasound for materials synthesis. In sonochemistry, ultrasound directly induces chemical reactions; while in USP, sonication does not produce chemical species and therefore does not cause chemical reactions. In fact, ultrasonic vibrations at the liquid surface are used to generate isolated microdroplets due to surface capillary waves.[3] These microdroplets act as individual microreactors with a series of *thermally driven* reactions occurring inside microdroplets as they flow through a heated oven. The applications of USP for nanostructured materials synthesis have been reviewed elsewhere.[3]

4. Combined chemical and physical effects for ultrasonic synthesis of nanomaterials

Under certain conditions, both the chemical and physical effects of high intensity ultrasound can play a synergistic role in the synthesis of nanomaterials. The application of the physical effects of ultrasound on the preparation of graphene was described in Section 2, but the chemical effects of ultrasound can also be exploited to aid in the preparation of functionalized graphenes. Recent work has shown that the use of a reactive solvent, such as styrene, that can be sonochemically activated allows for the relatively facile production of polymer functionalized single and few-layer graphenes in a single step.[76] During ultrasonic irradiation of graphite in styrene, polystyrene radicals will form and attack the surface of the exfoliated graphenes to form functionalized graphenes. Alternatively, the surface of graphite may first be functionalized by the radicals followed by exfoliation and further functionalization of the newly exposed graphene face will occur (Fig. 18). TEM images of graphenes prepared in this way are shown in Fig. 19. Sonication of a solution containing poly(vinyl alcohol) and graphite also led to the formation of polymer functionalized graphenes.[77] The functionalization was achieved *via* sonochemical degradation of poly(vinyl alcohol) to form macroradicals which then grafted onto graphene surfaces.

Another notable example of the application of both chemical and physical effects of high intensity ultrasound in materials synthesis is the preparation of protein microspheres. Sonication of a protein solution (*e.g.*, serum albumins) led to the formation of microcapsules which can contain gas or nonaqueous

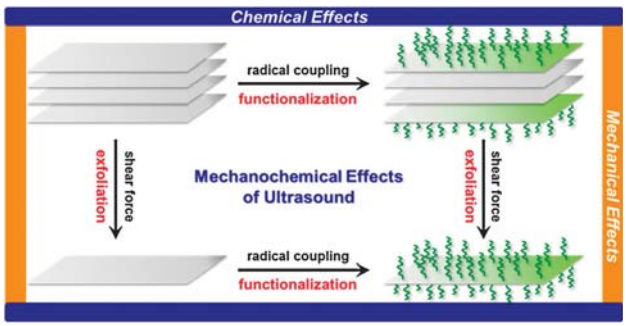

Fig. 18 Schematic illustration of the mechanochemical effects of ultrasound for the synthesis of polymer functionalized graphenes. Reprinted with permission from ref. 76. Copyright 2011 American Chemical Society.

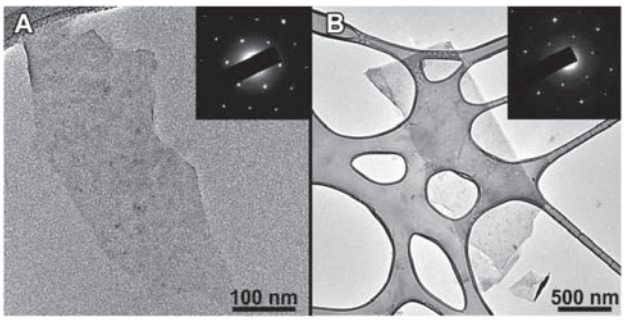

Fig. 19 TEM images of (A) single-layer graphene and (B) trilayer graphene with SAED insets confirming single-layer and few-layer graphenes, respectively. Reprinted with permission from ref. 76. Copyright 2011 American Chemical Society.

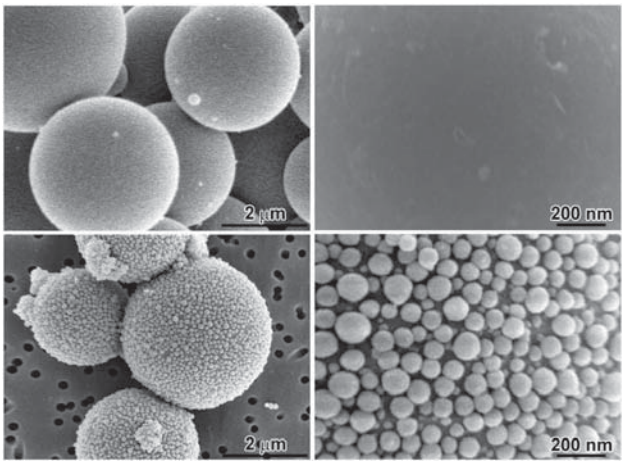

Fig. 20 SEM images of sonochemically prepared protein microspheres before and after nanoparticle functionalization by layer-by-layer adhesion: upper left, native microspheres as prepared by sonication of bovine serum albumin and upper right, close-up of the surface; lower left, silica-coated microspheres using a RGD polylysine peptide to reverse surface charge and lower right, close-up of its surface. Reprinted with permission from ref. 80. Copyright 2006 American Chemical Society.

liquid and whose surfaces are easily modified (Fig. 20).[78–80] The mechanism responsible for the formation of protein microspheres involves two acoustic phenomena: emulsification (a physical effect) and cavitation (and the subsequent chemical effects). Sonication creates an emulsion with proteins in the interface of two liquid phases. However, emulsification alone is not enough to prepare stable protein microspheres. Radicals (*e.g.*, $HO_2^{\bullet}$) produced *via* the sonolysis of water induce the cross-linking of the disulphide bonds between cysteine amino acid residues. The protein microspheres can also be modified after sonochemical preparation, for example with conjugation of cancer-cell selective ligands (*e.g.*, folate, monoclonal antibodies, RGD peptides, mercaptoethane sulphonate) to their surface.[80,81] Similar procedures can be used to prepare polysaccharide-based microspheres, for example, chitosan microspheres have been prepared in a single-step using sonochemical method.[82] The intermolecular imine cross-linking is important to the stabilization of the chitosan microspheres.

These protein microspheres have a wide range of clinical applications. Their use as echo contrast agents for improved sonography (*e.g.*, echocardiography) has become standard.[83] Protein microspheres have also been developed as ^{19}F-MRI contrast agents,[84] as *in vivo* MRI temperature probes,[85] as optical coherence tomography contrast agents,[86] for encapsulation and drug release,[87–89] and as multifunctional, multimodal cancer imaging contrast agents.[90]

The combination of chemical and physical effects of ultrasound can also be applied to prepare organic latex beads in a one-pot fashion. Through intense turbulence, ultrasound will create an emulsion of organic monomer in an aqueous medium. The radicals formed by sonolysis of water can diffuse into the organic phase to initiate the polymerization process. No additional initiators are required in this approach. In this method, fluorescent or magnetic substances can be incorporated into the latex particles to prepare functional latex beads.[91,92] For example, magnetic latex beads with a high content of magnetic nanoparticles have been prepared by ultrasonic irradiation of an emulsion of magnetite nanoparticles, surfactants, water and a reactive monomer.[92] Short sonication of this solution results in the formation of an emulsion of monomer loaded with magnetite nanoparticles stabilized by surfactants in the aqueous phase. Continuous sonication initiates the polymerization of the monomers to form latex particles.

5. Conclusions

High intensity ultrasound is responsible for a number of physical and chemical effects that are conducive to the preparation or modification of nanomaterials. The diverse mechanisms of action make it a powerful tool relevant to a large number of topics of current interest, including graphene, polymers, metal and metal oxide catalysts, crystallization, and anisotropic materials. With simple variations of reaction conditions and precursor compositions, a myriad of nanostructured materials with controlled morphologies, structures, and compositions have been successfully prepared by the application of high intensity ultrasound.

Acknowledgements

This work was supported by the NSF (DMR 09-06904). KSS would like to dedicate this paper to his mentors, Professors James P. Collman, John I. Brauman, and Robert G. Bergman, on the occasion of their 80th, 75th, and 70th birthdays, respectively.

References

1 K. S. Suslick, *Ultrasound: Its Chemical, Physical, and Biological Effects*, Wiley-VCH, New York, 1988.
2 K. S. Suslick and G. J. Price, *Annu. Rev. Mater. Sci.*, 1999, **29**, 295.
3 J. H. Bang and K. S. Suslick, *Adv. Mater.*, 2010, **22**, 1039.
4 K. S. Suslick, *Science*, 1990, **247**, 1439.
5 J. L. Luche, *Synthetic Organic Chemistry*, Plenum, New York, 1998.
6 T. J. Mason and J. P. Lorimer, *Applied Sonochemistry: The Uses of Power Ultrasound in Chemistry and Processing*, Wiley-VCH, Weinheim, 2002.

7 D. Chen, S. K. Sharma and A. Mudhoo, *Handbook on Applications of Ultrasound: Sonochemistry for Sustainability*, CRC Press, 2011.
8 *Theoretical and Experimental Sonochemistry Involving Inorganic Systems*, ed. Pankaj and M. Ashokkumar, Springer, 2010.
9 D. G. Shchukin, D. Radziuk and H. Mohwald, *Annu. Rev. Mater. Res.*, 2010, **40**, 345.
10 K. S. Suslick and D. J. Flannigan, *Annu. Rev. Phys. Chem.*, 2008, **59**, 659.
11 K. S. Suslick, *Sci. Am.*, 1989, **260**, 80.
12 C. R. Brenner, *Cavitation and Bubble Dynamics*, Oxford University Press, Oxford, 1995.
13 T. G. Leighton, *The Acoustic Bubble*, Academic Press, London, 1994.
14 J. R. Blake and D. C. Gibson, *Annu. Rev. Fluid Mech.*, 1987, **19**, 99.
15 C. D. Ohl, T. Kurz, R. Geisler, O. Lindau and W. Lauterborn, *Philos. Trans. R. Soc., London, Ser. A*, 1999, **357**, 269.
16 S. J. Doktycz and K. S. Suslick, *Science*, 1990, **247**, 1067.
17 T. Prozorov, R. Prozorov and K. S. Suslick, *J. Am. Chem. Soc.*, 2004, **126**, 13890.
18 K. S. Suslick, E. B. Flint, M. W. Grinstaff and K. A. Kemper, *J. Phys. Chem.*, 1993, **97**, 3098.
19 W. B. McNamara, Y. T. Didenko and K. S. Suslick, *Nature*, 1999, **401**, 772.
20 K. S. Suslick, S. B. Choe, A. A. Cichowlas and M. W. Grinstaff, *Nature*, 1991, **353**, 414.
21 M. W. Grinstaff, A. A. Cichowlas, S. B. Choe and K. S. Suslick, *Ultrasonics*, 1992, **30**, 168.
22 K. S. Suslick, M. Fang and T. Hyeon, *J. Am. Chem. Soc.*, 1996, **118**, 11960.
23 R. Bellissent, G. Galli, T. Hyeon, S. Magazu, D. Majolino, P. Migliardo and K. S. Suslick, *Phys. Scr.*, 1995, **T57**, 79.
24 K. S. Suslick, T. Hyeon and M. Fang, *Chem. Mater.*, 1996, **8**, 2172.
25 M. M. Mdleleni, T. Hyeon and K. S. Suslick, *J. Am. Chem. Soc.*, 1998, **120**, 6189.
26 T. Hyeon, M. Fang and K. S. Suslick, *J. Am. Chem. Soc.*, 1996, **118**, 5492.
27 J. D. Oxley, M. M. Mdleleni and K. S. Suslick, *Catal. Today*, 2004, **88**, 139.
28 Y. Koltypin, X. Cao, R. Prozorov, J. Balogh, D. Kaptas and A. Gedanken, *J. Mater. Chem.*, 1997, **7**, 2453.
29 N. A. Dhas and K. S. Suslick, *J. Am. Chem. Soc.*, 2005, **127**, 2368.
30 J. H. Bang and K. S. Suslick, *J. Am. Chem. Soc.*, 2007, **129**, 2242.
31 N. Du, H. Zhang, B. D. Chen, J. B. Wu, X. Y. Ma, Z. H. Liu, Y. Q. Zhang, D. R. Yang, X. H. Huang and J. P. Tu, *Adv. Mater.*, 2007, **19**, 4505.
32 S. H. Jeong, J. H. Ko, J. B. Park and W. Park, *J. Am. Chem. Soc.*, 2004, **126**, 15982.
33 X. H. Sun, C. P. Li, N. B. Wong, C. S. Lee, S. T. Lee and B. K. Teo, *J. Am. Chem. Soc.*, 2002, **124**, 14856.
34 R. A. Caruso, M. Ashokkumar and F. Grieser, *Langmuir*, 2002, **18**, 7831.
35 Y. Mizukoshi, K. Okitsu, Y. Maeda, T. A. Yamamoto, R. Oshima and Y. Nagata, *J. Phys. Chem. B*, 1997, **101**, 7033.
36 S. Anandan, F. Grieser and M. Ashokkumar, *J. Phys. Chem. C*, 2008, **112**, 15102.
37 K. Vinodgopal, Y. He, M. Ashokkumar and F. Grieser, *J. Phys. Chem. B*, 2006, **110**, 3849.
38 K. Okitsu, K. Sharyo and R. Nishimura, *Langmuir*, 2009, **25**, 7786.
39 A. Sánchez-Iglesias, I. Pastoriza-Santos, J. Pérez-Juste, B. Rodríguez-González, F. J. García de Abajo and L. M. Liz-Marzán, *Adv. Mater.*, 2006, **18**, 2529.
40 L. P. Jiang, S. Xu, J. M. Zhu, J. R. Zhang, J. J. Zhu and H. Y. Chen, *Inorg. Chem.*, 2004, **43**, 5877.
41 J. Zhang, J. Du, B. Han, Z. Liu, T. Jiang and Z. Zhang, *Angew. Chem., Int. Ed.*, 2006, **45**, 1116.
42 H. X. Xu and K. S. Suslick, *ACS Nano*, 2010, **4**, 3209.
43 B. T. Mayers, K. Liu, D. Sunderland and Y. N. Xia, *Chem. Mater.*, 2003, **15**, 3852.
44 J. J. Zhu, S. Xu, H. Wang, J. M. Zhu and H. Y. Chen, *Adv. Mater.*, 2003, **15**, 156.
45 T. Gao and T. Wang, *Chem. Commun.*, 2004, 2558.
46 P. Hasin and Y. Y. Wu, *Chem. Commun.*, 2012, **48**, 1302.
47 V. G. Pol, A. Gedanken and J. Calderon-Moreno, *Chem. Mater.*, 2003, **15**, 1111.
48 V. G. Pol, H. Grisaru and A. Gedanken, *Langmuir*, 2005, **21**, 3635.
49 H. B. Pan and C. M. Wai, *New J. Chem.*, 2011, **35**, 1649.
50 K. Vinodgopal, B. Neppolian, I. V. Lightcap, F. Grieser, M. Ashokkumar and P. V. Kamat, *J. Phys. Chem. Lett.*, 2010, **1**, 1987.
51 S. H. Jung, E. Oh, K. H. Lee, W. Park and S. H. Jeong, *Adv. Mater.*, 2007, **19**, 749.
52 K. Chatakondu, M. L. H. Green, M. E. Thompson and K. S. Suslick, *Chem. Commun.*, 1987, 900.
53 J. E. Jones, M. C. Cheshire, D. J. Casadonte and C. C. Phifer, *Org. Lett.*, 2004, **6**, 1915.
54 J. Walter, M. Nishioka and S. Hara, *Chem. Mater.*, 2001, **13**, 1828.
55 L. M. Viculis, J. J. Mack and R. B. Kaner, *Science*, 2003, **299**, 1361.
56 Y. Hernandez, V. Nicolosi, M. Lotya, F. M. Blighe, Z. Sun, S. De, I. T. McGovern, B. Holland, M. Byrne, Y. K. Gun'Ko, J. J. Boland, P. Niraj, G. Duesberg, S. Krishnamurthy, R. Goodhue, J. Hutchison, V. Scardaci, V. A. C. Ferrari and J. N. Coleman, *Nat. Nanotechnol.*, 2008, **3**, 563.
57 J. N. Coleman, M. Lotya, A. O'Neill, S. D. Bergin, P. J. King, U. Khan, K. Young, A. Gaucher, S. De, R. J. Smith, I. V. Shvets, S. K. Arora, G. Stanton, H. Y. Kim, K. Lee, G. T. Kim, G. S. Duesberg, T. Hallam, J. J. Boland, J. J. Wang, J. F. Donegan, J. C. Grunlan, G. Moriarty, A. Shmeliov, R. J. Nicholls, J. M. Perkins, E. M. Grieveson, K. Theuwissen, D. W. McComb, P. D. Nellist and V. Nicolosi, *Science*, 2011, **331**, 568.
58 T. Prozorov, B. McCarty, Z. Cai, R. Prozorov and K. S. Suslick, *Appl. Phys. Lett.*, 2004, **85**, 3513.
59 T. Prozorov, R. Prozorov, A. Snezhko and K. S. Suslick, *Appl. Phys. Lett.*, 2003, **83**, 2019.

60 H. M. Xiong, D. G. Shchukin, H. Mohwald, Y. Xu and Y. Y. Xia, *Angew. Chem., Int. Ed.*, 2009, **48**, 2727.
61 V. Belova, T. Borodina, H. Mohwald and D. G. Shchukin, *Ultrason. Sonochem.*, 2011, **18**, 310.
62 D. V. Andreeva, D. Fix, H. Mohwald and D. G. Shchukin, *Adv. Mater.*, 2008, **20**, 2789.
63 J. C. Yu, J. Yu, W. Ho and L. Zhang, *Chem. Commun.*, 2001, 1942.
64 D. Qian, J. Z. Jiang and P. L. Hansen, *Chem. Commun.*, 2003, 1078.
65 J. Geng, J. J. Zhu, D. J. Lu and H. Y. Chen, *Inorg. Chem.*, 2006, **45**, 8403.
66 A. M. Basedow and K. Ebert, *Adv. Polym. Sci.*, 1977, **22**, 83.
67 C. R. Hickenboth, J. S. Moore, S. R. White, N. R. Sottos, J. Baudry and S. R. Wilson, *Nature*, 2007, **446**, 423.
68 J. M. Paulusse and R. P. Sijbesma, *Angew. Chem., Int. Ed.*, 2004, **43**, 4460.
69 M. J. Kryger, M. T. Ong, S. A. Odom, N. R. Sottos, S. R. White, T. J. Martinez and J. S. Moore, *J. Am. Chem. Soc.*, 2010, **132**, 4558.
70 K. L. Berkowski, S. L. Potisek, C. R. Hickenboth and J. S. Moore, *Macromolecules*, 2005, **38**, 8975.
71 K. M. Wiggins, T. W. Hudnall, Q. Shen, M. J. Kryger, J. S. Moore and C. W. Bielawski, *J. Am. Chem. Soc.*, 2010, **132**, 3256.
72 J. N. Brantley, K. M. Wiggins and C. W. Bielawski, *Science*, 2011, **333**, 1606.
73 B. W. Zeiger and K. S. Suslick, *J. Am. Chem. Soc.*, 2011, **133**, 14530.
74 D. K. Bucar and L. R. MacGillivray, *J. Am. Chem. Soc.*, 2007, **129**, 32.
75 J. R. G. Sander, D. K. Bucar, J. Baltrusaitis and L. R. MacGillivray, *J. Am. Chem. Soc.*, 2012, **134**, 6900.
76 H. X. Xu and K. S. Suslick, *J. Am. Chem. Soc.*, 2011, **133**, 9148.
77 B. Shen, W. T. Zhai, D. D. Lu, J. Wang and W. G. Zheng, *RSC Adv.*, 2012, **2**, 4713.
78 K. S. Suslick and M. W. Grinstaff, *J. Am. Chem. Soc.*, 1990, **112**, 7807.
79 M. W. Grinstaff and K. S. Suslick, *Proc. Natl. Acad. Sci. U. S. A.*, 1991, **88**, 7708.
80 F. J.-J. Toublan, S. Boppart and K. S. Suslick, *J. Am. Chem. Soc.*, 2006, **128**, 3472.
81 D. Baram-Pinto, S. Shukla, M. Richman, A. Gedanken, S. Rahimipour and R. Sarid, *Chem. Commun.*, 2012, **48**, 8359.
82 N. Skirtenko, T. Tzanov, A. Gedanken and S. Rahimipour, *Chem.–Eur. J.*, 2010, **16**, 562.
83 S. P. Qin, C. F. Caskey and K. W. Ferrara, *Phys. Med. Biol.*, 2009, **54**, R27–R57.
84 A. G. Webb, M. Wong, K. J. Kolbeck, R. L. Magin, L. J. Wilmes and K. S. Suslick, *J. Magn. Reson. Imaging*, 1996, **6**, 675.
85 K. J. Liu, M. W. Grinstaff, J. Jiang, K. S. Suslick, H. M. Swartz and W. Wang, *Biophys. J.*, 1994, **67**, 896.
86 S. A. Boppart and K. S. Suslick, in *Optical Coherence Tomography in Cardiovascular Research*, ed. E. Regar, T. G. van Leeuwen and P. Serruys, CRC Press, 2007, ch. 29, pp. 267–281.
87 R. Silva, H. Ferreira and A. Cavaco-Paulo, *Biomacromolecules*, 2011, **12**, 3353.
88 E. K. Skinner and G. J. Price, *Chem. Commun.*, 2012, **48**, 9260.
89 N. Skirtenko, M. Richman, Y. Nitzan, A. Gedanken and S. Rahimipour, *Chem. Commun.*, 2011, **47**, 12277.
90 R. John, F. T. Nguyen, K. J. Kolbeck, E. J. Chaney, M. Marjanovic, K. S. Suslick and S. A. Boppart, *Mol. Imaging Biol.*, 2012, **14**, 17.
91 M. Bradley, M. Ashokkumar and F. Grieser, *J. Am. Chem. Soc.*, 2003, **125**, 525.
92 B. M. Teo, F. Chen, T. A. Hatton, F. Grieser and M. Ashokkumar, *Langmuir*, 2009, **25**, 2593.